ISSN 2029-6991 / eISSN 2029-7009

VILNIUS TECH
Vilnius Gediminas Technical University

GEODESY and CARTOGRAPHY

2025
Volume 51
Issue 2
Pages 107–114
https://doi.org/10.3846/gac.2025.21128

UDC 528.54

ACCURACY TEST OF SATELLITE IMAGERY-DERIVED BATHYMETRY IN SHALLOW WATERS USING SENTINEL-2A MULTISPECTRAL IMAGERY

Rizqi Rizaldi HIDAYAT[1]✉, Amron AMRON[1], Iqbal Ali HUSNI[1], Isnaini PRIHATININGSIH[1], Hartoyo HARTOYO[1], Mukti TRENGGONO[1], Muhammad Romdonul HAKIM[2]

[1]*Department of Marine Science, Jenderal Soedirman University, Purwokerto, Indonesia*
[2]*Pangandaran Marine and Fisheries Polytechnic, Pangandaran, Indonesia*

Article History:
- received 11 March 2024
- accepted 28 May 2025

Abstract. Continuous bathymetry mapping for shallow waters is very important considering that these waters are prone to change. Bathymetry measurements obtained from satellite imagery are an alternative that can be used. This study aimed to evaluate and develop algorithms that can be used to estimate shallow water depth values obtained from satellite imagery. In this study, the depth mapping results were obtained from Surface Reflectance derived from Sentinel-2A image processing. A comparative analysis was performed by comparing measurements obtained with an echosounder and estimated depths estimated with Lyzenga, Stumpf, and modified Stumpf algorithms. In this study, where the depth ranged from 2–6 meters, the Lyzenga algorithm performed the best algorithm with the R^2 value of 0.94 and the RMSE 0.23, followed by the modified Stumpf algorithm with an R^2 value of 0.93 and RMSE 0.24, and Stumpf algorithm with a R^2 value of 0.88 and a RMSE of 0.32. Overall, this study provides an important contribution to comparing Lyzenga and Stumpf algorithms for estimating water depths. This study provides guidance on choosing the correct algorithm for bathymetric mapping using satellite imagery in similar water locations.

Keywords: satellite derived bathymetry, shallow water, Google Earth Engine, satellite imaging, Sentinel-2A, statistical modelling.

✉Corresponding author. E-mail: *rizqi.rizaldi@unsoed.ac.id*

1. Introduction

Bathymetry mapping is the process of measuring and visualizing ocean depths. This process has an important role in understanding and managing marine resources, especially in shallow water areas. The shallow water area is one of the most dynamic and rapidly changing environments. Intensive and frequent changes in this coastal area demand an efficient monitoring method that can produce repeated updates of seafloor topography and bathymetry information. Bathymetry information in shallow water areas is needed in various ways such as tsunami propagation modeling (Poliyapram et al., 2017), waste distribution modeling (Jeyar et al., 2015), shipping safety (Seto & Crawford, 2016), and coastal environmental management. A bathymetry map is used to plan coastal infrastructure developments, such as wharves, embankments, or waterways. In conventional bathymetry methods such as using an echosounder, bathymetry measurements take a long time (Parente & Vallario, 2019). The availability of open-access satellite imagery with high spatial resolution such as Sentinel-2 and cloud-based computing platforms such as Google Earth Engine (GEE), makes the use of satellite imagery an attractive alternative in bathymetric mapping in shallow water areas (Muzirafuti et al., 2020; Sagawa et al., 2019; Said et al., 2017).

Satellite Derived Bathymetry (SDB) uses satellite image data and image processing techniques to extract water depth information. This method utilizes the characteristics of light reflected from the seabed and complex processing processes to produce accurate depth estimates (Lyzenga, 1978). In recent years, SDB has become an interesting research topic and has been shown to provide competitive results compared to conventional methods (Al Najar et al., 2021; Cesbron et al., 2021; Duplančić Leder et al., 2023). Bathymetry mapping using SDB has several advantages. The use of satellite imagery allows extensive and continuous bathymetry mapping in shallow water areas which include coastal waters, estuaries and coral reefs (Westley, 2021). This provides a more comprehensive picture of the structure of the seafloor and the aquatic environment as a whole. With SDB, bathymetry mapping can be faster, more accurate and more cost-effective (Duplančić Leder et al., 2023). The use of satellite imagery allows water areas to be mapped quickly without deploying ships or special equipment. The service is especially useful in emergency situations or when bathymetric mapping needs to be done quickly to support marine activities like navigation, research, and natural resource management.

Several algorithms have been developed for the SDB method, both empirically and physics-based approaches. The empirical approach is the most widely used. An empirical approach is made based on the statistical relationship between known depth data and Rrs (λ) measurements in one or several bands (Wei et al., 2020). The main advantage of empirical approaches is the ability to retrieve water depths relatively easily, but their reliance on calibration from field observations. This approach is easy to implement using multi-spectral satellite imagery. Some of the most widely used empirical approach algorithms are Lyzenga (Lyzenga, 1978) and Stumpf (Stumpf et al., 2003).

In specific cases, the existing SDB algorithm must be adapted and modified according to the special characteristics and conditions at the new location. Each water location can have variations in light, seafloor substrate, and other environmental conditions that can affect the estimated depth. The characteristics of the waters in the study area are dominated by total suspended solids, with concentrations ranging from 8–9 mg/L (Hidayat et al., 2023). The substrate in the area is a muddy sand base with no aquatic vegetation, such as seagrass or seaweed. Therefore, it is necessary to conduct additional adjustments and validations to ensure the accuracy of the estimation at the new location. This study aims to compare several algorithms commonly used in the SBD method and modify the algorithm so that it is suitable for bathymetric mapping in the study area.

2. Study area

Figure 1 illustrated the research location on the north coast of Java Island, precisely in Kaliwungu waters, Kendal, Central Java, which is geographically located at 6.9375–6.9023 °S, 110.2907–110.3268 °E. These waters are included in the category of shallow waters with a depth of 0–6 meters and relatively in a calm conditions, constant wave and current conditions according to the season. The area around the research location is saturated with plywood mills, so ships transporting or pulling wood often pass through it. The concentration of total suspended matter around the study site ranged from 9–106 mg/L and the concentration of Chlorophyll-a ranged from 1–9 mg/m^3 (Maslukah et al., 2022). According to Yuliastini et al. (2023), the Kaliwungu coast is classified as moderate vulnerability with a Coastal Vulnerability Index (CVI) of 21.38.

3. Data and methods

3.1. Tools and materials

This research used Sentinel-2 imagery which is available for free on the GEE platform. Although the Sentinel-2 image has many bands, we only captured the blue (B2), green (B3), red (B4), and near-infrared/NIR (B8) bands. GEE provides two types of Sentinel-2 images, namely: (1) Level-1C orthorectified top-of-atmosphere reflectance (TOA), an

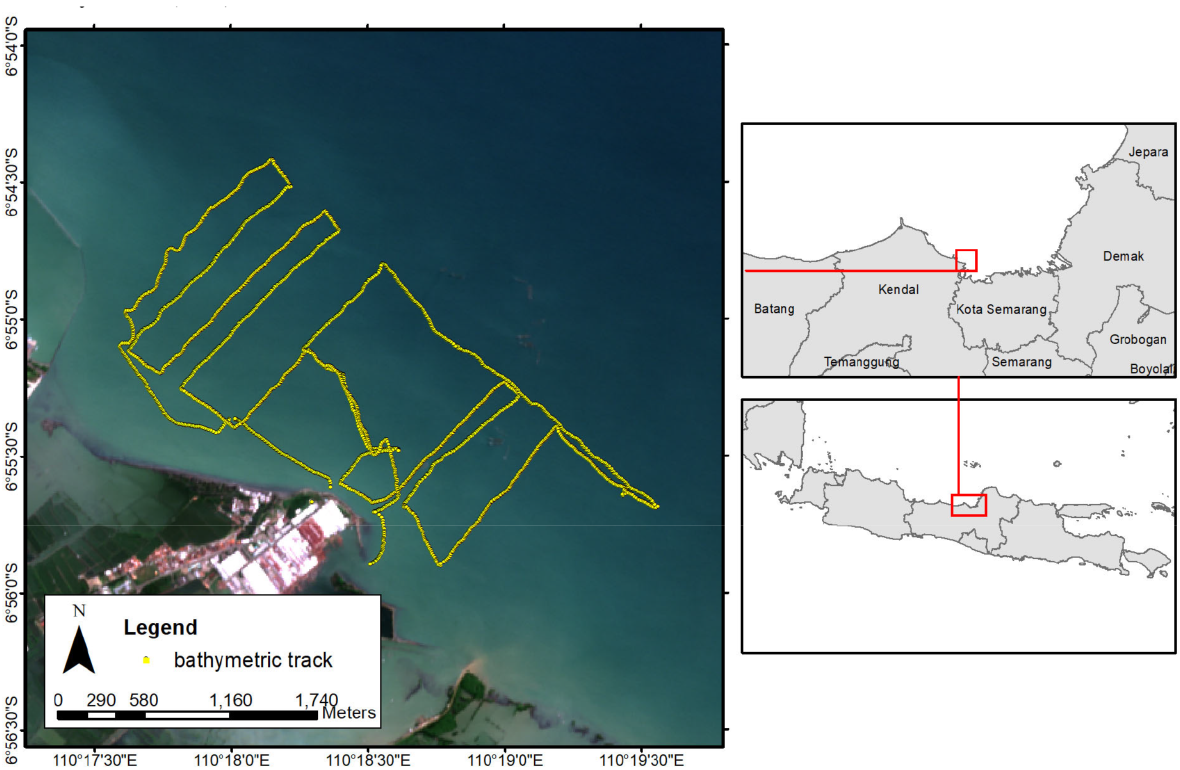

Figure 1. Research location for bathymetric model analysis. The image is a Sentinel-2 image composite used for analysis

image that describes the reflectance of sunlight reaching the upper atmosphere and reflection from the ground surface. This image needs further processing to reduce the influence of the atmosphere to produce an atmospherically corrected image. (2) Level-2A orthorectified atmospherically corrected surface reflectance (SR) or Bottom-of-Atmosphere (BOA), images that have gone through atmospheric correction and provide reflectance values that are reflected directly by objects on the earth's surface. Shallow water areas often have high levels of turbidity, which can affect the absorption and scattering of light by the water. The use of SR imagery can provide more accurate information about the amount of light reflected by the water surface (Kuhn et al., 2019). This study uses harmonized SR imagery (S2_SR_HARMONIZED). Harmonized images are images that have gone through a normalization process to eliminate atmospheric and instrument differences between various images taken at different times and conditions. These images provide consistency of image values over time and allow for more accurate comparison and analysis between images. Harmonized Sentinel-2 product, integrates L8/OLI and S2/MSI input data into a consistent data set with higher temporal frequencies (2–4 days) and standard spatial resolution (Chaves et al., 2020).

Several factors are considered when selecting an image from the cloud, including cleanliness and recording time. The image recording time determines the depth correction value between high and low tide when field data is collected. Six Sentinel-2 scenes at different times are composited and the average value for each band is calculated (Table 1).

Satellite image processing was conducted using Google Earth Engine. This platform was chosen for its robust capabilities in handling large geospatial datasets and applying complex image analysis algorithms. For testing accuracy, RStudio was utilized to calculate performance metrics such as coefficient of determination (R^2) and Root Mean Square Error (*RMSE*). Map visualization was performed using ArcGIS software.

3.2. Field data acquisition

In situ bathymetry data from the sounding results were used to train, validate, and test the SDB model. A total of 300 points were used for training and validation, and 100 points were used for accuracy testing. The data was obtained using the Garmin GPSmap 585 Sounder, which operated using a dual-frequency (50/200 kHz) transducer and equipped with a Garmin GPS antenna. This type of echo sounder is widely used for bathymetry measurements (Kumaat et al., 2021; Lubis et al., 2020; Purba et al., 2022). The total route was 20 km with a total of more than 2000 points and the average distance between points was 15 meters.

The sounding data was extracted into xyz format where the x and y values indicate the coordinate position, while the z value indicates the depth value. The data was previously corrected with tidal data and the depth of the transducer installation. Based on tidal data for 15 days, it is known that the sounding was done when the tide is between –0.03 and 0.13 meters. The depth data from echosounder measurements is reduced by the tides using Equation ((1)).

$$r_t = TWL_t - \left(MSL + Z_0\right). \tag{1}$$

In this equation, r_t – the magnitude of the reduction (correction) given to the measurement value at time t, TWL_t – the true water level at time t, MSL – the mean sea level, and Z_0 – low tide depth below MSL. Then, the actual depth value was determined using Equation ((2)):

$$D = dT - r_t, \tag{2}$$

where D – actual depth, dT – transducer corrected depth, and r_t – ocean tide reduction. Then, the actual depth point values that have been scattered were processed using mapping software to be interpolated. Interpolation is the process of predicting the value at a point that is not a sample point, based on the value of the surrounding points that are sampled. Interpolation returns values for locations where data is not available. The interpolation method used in this study is Kriging. Kriging is recognized as superior for constructing bathymetric data compared to other interpolation methods such as Inverse Distance Weighting (IDW) (Ferreira et al., 2017). The Kriging process was conducted with a grid resolution that adjusts the spatial resolution of the Sentinel-2 imagery, which is 10 meters.

3.3. Satellite image processing

The processing stage was begun with separating land and sea (masking). This stage aims to prevent the land area from being processed when entering the shallow water bathymetry algorithm. Masking process conducted with Normalized Difference Water Index (NDWI) algorithm,

Table 1. Sentinel-2 image used for analysis

Id Image	Time (UTC+7)	Tide (m)
20210421T024541_20210421T025916_T49MDN	21 April 2021 09:45:41	–0.03
20210423T023539_20210423T025728_T49MDN	23 April 2021 09:45:39	–0.02
20210426T024539_20210426T030731_T49MDN	26 April 2021 09:45:39	0.12
20210511T024551_20210511T025920_T49MDN	11 May 2021 09:45:51	0.18
20210516T024549_20210516T025931_T49MDN	16 May 2021 09:45:49	0.26
20210521T024551_20210521T025921_T49MDN	21 May 2021 09:45:51	0.03

which assesses the wettability of an area by comparing the values of the green reflectance band (B3) and the near infrared band (B8) (McFeetters, 1996). This algorithm has been widely used to separate terrestrial and aquatic (Aryal et al., 2021; Cordeiro et al., 2021; Ngoc et al., 2019). The algorithm from NDWI is given in Equation ((3)).

$$NDWI = \frac{B3 - B8}{B3 + B8}. \tag{3}$$

A total of 70% of the 300 points used for training were selected to represent various depth values. These points were used to study the relationship between the input variable (reflectance values from satellite images in each band) and the output variable (bathymetry values). Through several iterations, the model adjusted its parameters to minimize prediction error. The remaining 30% of the points were used for model validation. This process was carried out to prevent overfitting, where the model may perform well on training data but not on new data.

The depth values were obtained using several commonly used algorithms and modified algorithm developed by the author. The first algorithm is Lyzenga (1985). Sea surface radiation is the result of bottom reflection and light attenuation through the water column underlies the development of the Lyzenga algorithm (Rossi et al., 2020). The approach considers light attenuation exponential relationship with water depth and uses a linear transformation function to relate observed reflectance values to water depth. This model uses linear regression to obtain shallow water depth values from multispectral images, so it is also called a linear algorithm. The Lyzenga algorithm is widely applied to shallow water areas (Aulia et al., 2020; Prasetya et al., 2023; Westley, 2021). The Lyzenga algorithm used is described in Equation ((4).

$$Z = m_0 + \sum_{t=1}^{3} m_1 R_t. \tag{4}$$

In this equation, Z – depth of prediction in meters, m_0 = constant or regression intercept, m_1 – regression coefficient in each band, and R_t – reflectance value of each band. The constants m_0 and m_1 are obtained from the results of analysis using multivariate regression. We use a combination of the three bands Red, Green, and Blue so that we can produce an R^2 of 0.93 and an RSME of 0.26 meters. The regression equation becomes as follows:

$$Z = 6.7863 - 0.0064\, R_{red} - 0.0136\, R_{green} + 0.0159\, R_{blue}. \tag{5}$$

The Stumpf Algorithm (Stumpf et al., 2003) was applied for the second algorithm. This model assumes that reflections on certain band absorb more slowly than reflections from other bands. Consequently, the ratio of the high absorption band to the low absorption band will display a linear decrease with depth when both are log-transformed. This algorithm is also known as the Ratio Algorithm because it uses the ratio of observed object reflections and two constants that can be adjusted to get the water depth (Equation ((6)).

$$Z = m_1 \times \frac{\ln(R_b)}{\ln(R_g)} - m_0, \tag{6}$$

where Z – the prediction depth in meters, m_1 and m_0 are constants and regression intercept, R_b – the reflectance value in the blue band, and R_g – the reflectance value in the green or red band. The combination of the Blue and Green bands gives an R^2 value of 0.89, an RMSE of 0.32 meters, and Equation (7):

$$Z = 144.3 \times \frac{\ln(R_{blue})}{\ln(R_{green})} - 137.2. \tag{7}$$

The Stump Algorithm was modified by including the Red channel, which produces a better R^2 value, 0.93, and RMSE of 0.26. The modified equation becomes Equation (8):

$$Z = 173.9 \times \frac{\ln(R_{blue})}{\ln(R_{red}) + \ln(R_{green})} - 85.14. \tag{8}$$

3.4. Accuracy test

An accuracy test was conducted to assess the performance of the developed model. This test involved comparing the actual depth values with the model's predicted depth values. The evaluation was performed using 100 points different from those used in the training and validation processes. To evaluate the accuracy of the bathymetric estimation, we use the coefficient of determination/ R^2 (Equation ((9)) nd Root Mean Square Error/ $RMSE$ (Equation ((10)).

$$R^2 = 1 - \frac{\sum_{i=1}^{n} \left(Z_{pre} - Z_{obs}\right)^2}{\sum_{i=1}^{n} \left(Z_{obs} - \overline{Z_{obs}}\right)^2}; \tag{9}$$

$$RMSE = \sqrt{\frac{\sum_{i=1}^{n} \left(Z_{obs} - Z_{pre}\right)^2}{n}}, \tag{10}$$

where n – the number of samples, Z_{pre} represents the predicted depth value in meters obtained from image processing, and Z_{obs} represents the sounding depth value in meters. R^2 is a statistical measure to assess how well a regression model makes predictions. This value provides information about the proportion of variance in the dependent variable that the independent variables can explain. R^2 values range from 0 to 1; the closer the value is to 1, the better the model describes the data variance. $RMSE$ is a metric used to measure the error level in a predictive model. In other words, $RMSE$ indicates the average difference between predicted and actual values. A lower $RMSE$ value indicates that the model has better accuracy in predicting the actual values.

4. Results and discussion

The GEE platform used in this study is a cloud-based geospatial analysis platform that allows fast processing of large data sets. Figure 2 depicts the bathymetry values in the study area. Bathymetry data from sounding results are interpolated to obtain a raster view of the depth from the points (Figure 2a). The results of the SDB model with three algorithms are shown in Figure 2b, 2c, 2d. Visually, all SDB models conform to the reference bathymetry images. Depth values can be estimated SDB, even in places where there is no data in the reference bathymetry images. Depth values in the study area are in the range of 0–8 meters with gently sloping seafloor contours.

Generally, the three SDB algorithm models successfully mapped bathymetry at the site. The Stumpf algorithm is simpler and easier during the processing stage. The basic principle of the Stumpf algorithm is that each band has a different absorption rate in the water body. This difference in absorption rate results in the ratio between the bands, which consistently changes along with the change in depth. Theoretically, an increase in band ratio would indicate an increase in depth (Said et al., 2017). The bands with higher absorption rates will continue to decrease as the depth increases. However, this model gives slightly grainy results compared to the Lyzenga model which has a cleaner finish. The Lyzenga algorithm requires more complicated techniques at the processing stage because this model applies the multiple regression method. The third algorithm which is a modified Stumpf algorithm produces results similar to Lyzenga algorithm but is easier to implement since linear regression is the only method used.

The results of the comparative analysis between the in-situ survey and the SDB have been presented in Figure 3. Figure 3 illustrates that the depth contour patterns are almost similar between the three methods. However, there are differences in the depth values generated using the Stumpf algorithm. In this case, the pattern formed by the Stumpf algorithm (blue line) appears to be unstable, with a tendency to over-estimate or under-estimate the depth value compared to the other two algorithms which tend to under-estimate the depth value. All three algorithms revealed larger errors for deeper points. The accuracy of bathymetry mapping with SDB is affected by the depth of the water. Duan et al. (2022) stated that the SDB model tends to provide

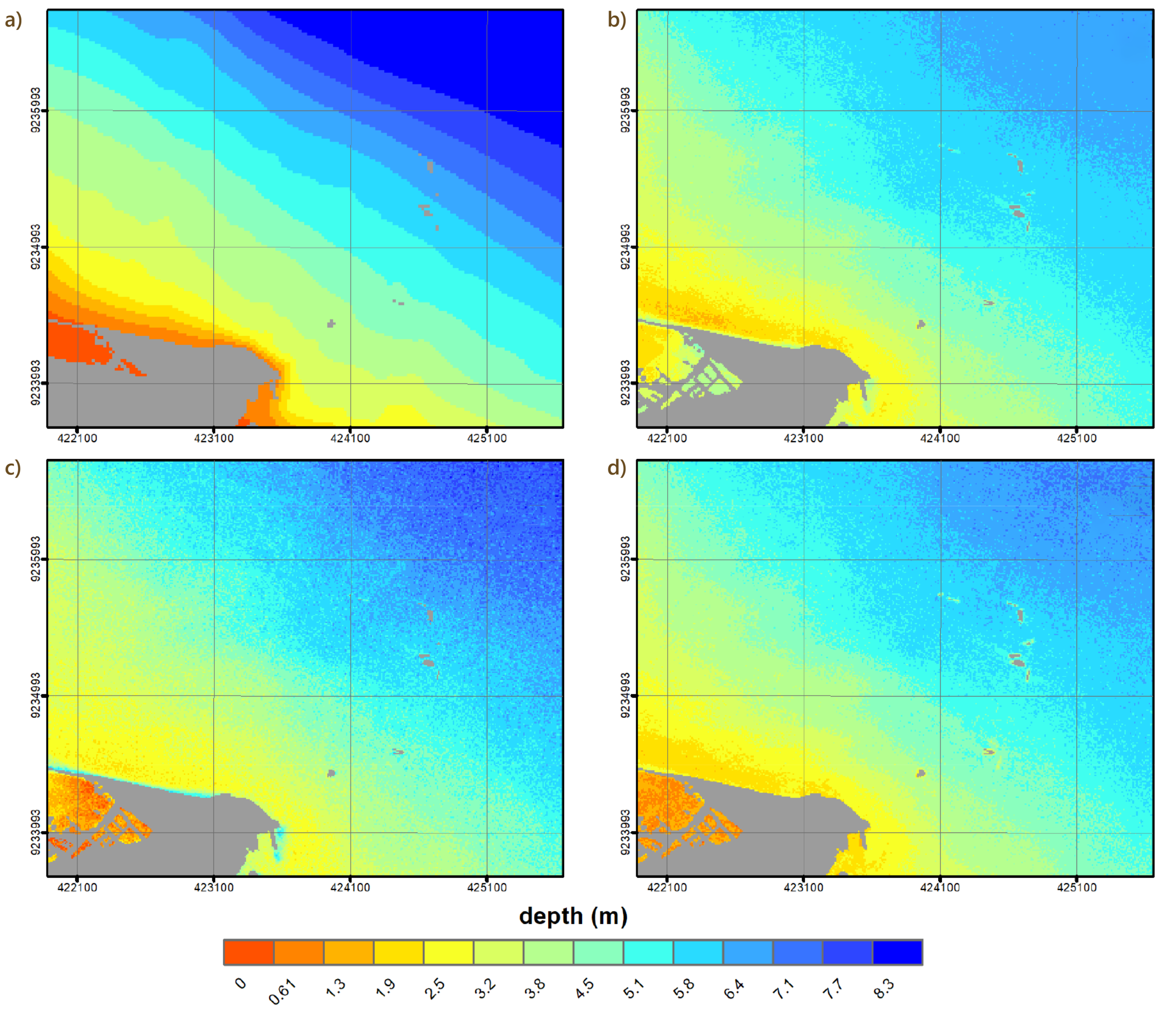

Figure 2. A depth value of in-situ data processing results and Sentinel-2 Imagery: a – results of in-situ data interpolation; b – SDB using the Lyzenga equation; c – SDB using the Stumpf equation; and d – SDB using the modified Stumpf equation

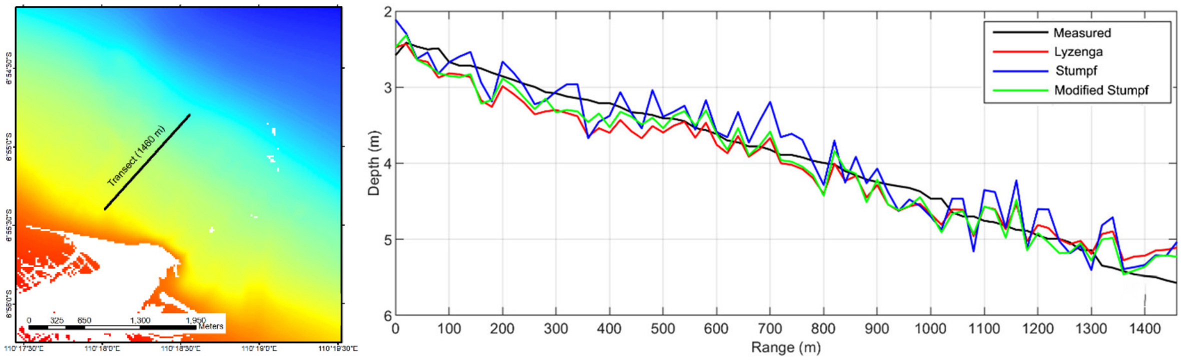

a) b)

Figure 3. The SDB profile uses three different algorithms compared to the depth profile survey results (b); a transect perpendicular to the coastline located in the middle of the study area (a)

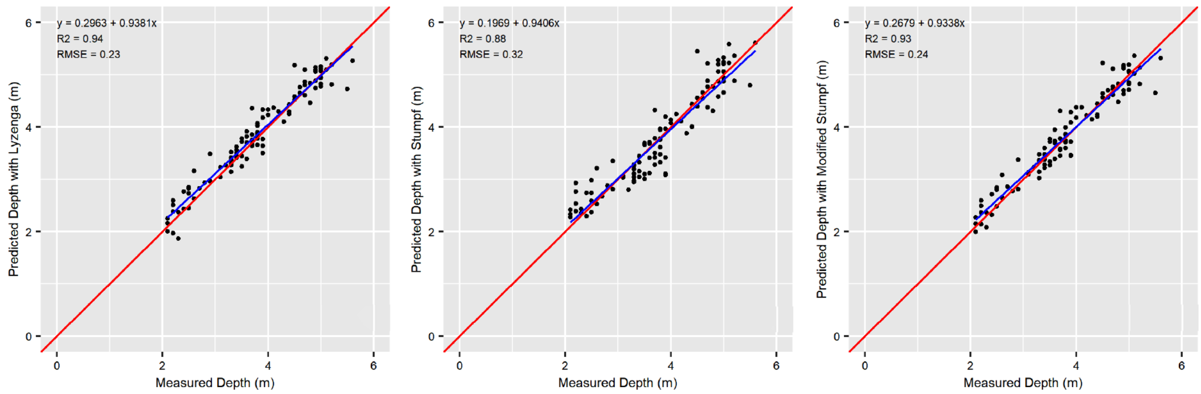

a) b) c)

Figure 4. Scatter plot validation of the predicted depth value (y-axis) against the depth of the in situ measurement results (x-axis), the 1:1 line is shown in red: a – implementation of Lyzenga (Equation (5)); b – implementation of Stumpf (Equation (7)); and c – implementation of modified Stumpf (Equation (8))

more precise results in shallow water areas, but has a significantly higher error rate in deeper waters.

According to Figure 4, all algorithm figures displayed a good linear trend. The best relation is shown by the Lyzenga algorithm (R^2 = 0.94), followed by the modified Stumpf algorithm (R^2 = 0.93), and the Stumpf algorithm (R^2 = 0.88). The RMSE value indicated that Lyzenga has the smallest error value, which was 0.23 m, followed by the modified Stumpf (0.24), and Stumpf (0.32). Lyzenga algorithm has been widely used in bathymetry mapping. The use of the Lyzenga algorithm in this study has the best accuracy value. These results were also found in a study conducted by (Rossi et al., 2020), in which the study compared the Lyzenga algorithm with other methods, where the Lyzenga algorithm produced the most accurate results.

The SDB algorithm is strongly influenced by the characteristics of the existing seafloor substrate. Several factors, such as sediment type, rock structure, and vegetation, significantly affect the depth estimation results produced by this algorithm. Different types of substrates can give different error values. The sand-based substrate type is the best type of substrate to apply SDB (Li et al., 2023). Sand has greater physical stability than mud. This minimizes the disturbance caused by water movement, providing more consistent data for the SDB algorithm to process. The seafloor substrate type in the study area is dominated by sand. Therefore all SDB model results have good accuracy (RMSE ≤ 0.32 m).

In addition, the content of both dissolved and undissolved particles also affects the results of estimating the depth value using the SDB method. There are several parameters that influence optical processes in water, including total suspended solids (TSS) and chlorophyll-a concentrations (Caballero et al., 2019; Mudiyanselage et al., 2022). High concentrations of TSS can trigger light scattering and absorption, reducing the ability of satellite imagery to obtain accurate information about the seafloor substrate. Meanwhile, the concentration of chlorophyll-a can affect the color of the water. The high concentration of chlorophyll-a in the waters can cause spectral changes in satellite images. An increase in chlorophyll-a content tends to give the water a greener or murkier color, which can affect the quality of satellite imagery. These spectral changes can affect the depth estimation using the SDB method. The presence of a higher concentration of suspended matter can affect the accuracy of the depth value and reduce the maximum depth limit that can be measured (Casal et al., 2020). In order to estimate water depth using SDB, other water parameters must be considered. However, the SDB algorithm can be used for a variety of applications, including maritime navigation, monitoring changes in wetlands, and understanding the dynamics of aquatic ecosystems. The SDB algorithm is expected to make a significant contribution to efficiently mapping and monitoring aquatic environments with advances in technology and analysis.

5. Conclusions

This paper compares the bathymetry values derived from satellite imagery in shallow waters obtained through three different algorithms. The results of this study provide knowledge about the effectiveness and accuracy of each algorithm in the context of bathymetric mapping using satellite imagery. The Lyzenga algorithm provides reliable estimates of shallow water depths, as indicated by its highest coefficient of determination. By exploiting a statistical relationship between the reflectance of light from the seafloor and the actual depth, this algorithm is able to provide accurate and consistent estimates. However, Lyzenga algorithm requires multiple regression analysis, which is quite challenging to implement. The algorithm that we developed from the modification of the Stumpf algorithm can be another alternative. This algorithm gives a coefficient of determination and error that is not much different from the Lyzenga algorithm.

Acknowledgements

This research was financially supported by LPPM Jenderal Soedirman University through the RPK scheme contract number 27.309/UN23.37/PT.01.03/II/2023. The authors would also like to thank PT Kayu Lapis Indonesia and PT Biosfer Saintek Indonesia for the support of facilities and equipment during the research.

Funding

This work was supported by the LPPM Jenderal Soedirman University under Grant 27.309/UN23.37/PT.01.03/II/2023.

Author contributions

Conceptualization, R. R. H. and A. A.; methodology, R. R. H. and A. A.; software, R. R. H; validation, A. A., I. A. H., and M. R. H.; formal analysis, R. R. H. and M. R. H.; investigation, I. P, H. H., and M. T.; resources, R. R. H., I. A. H., and M. R. H.; data curation, R. R. H., I. P., and M. T.; writing – original draft preparation, R. R. H., I. A. H, and I. P.; writing – review and editing, A. A., H. H., and M. T.; visualization, R. R. H. and M. R. H.; supervision, A. A., and M. T. All authors have read and agreed to the published version of the manuscript.

Disclosure statement

The authors declare no conflict of interest. The founding sponsors had no role in the design of the study; in the collection, analyses, or interpretation of data; in the writing of the manuscript, and in the decision to publish the results.

References

Al Najar, M., Thoumyre, G., Bergsma, E. W. J., Almar, R., Benshila, R., & Wilson, D. G. (2021). Satellite derived bathymetry using deep learning. *Machine Learning*, *112*(4), 1107–1130. https://doi.org/10.1007/s10994-021-05977-w

Aryal, B., Escarzaga, S. M., Vargas Zesati, S. A., Velez-Reyes, M., Fuentes, O., & Tweedie, C. (2021). Semi-automated semantic segmentation of arctic shorelines using very high-resolution airborne imagery, spectral indices and weakly supervised machine learning approaches. *Remote Sensing*, *13*(22), Article 4572. https://doi.org/10.3390/rs13224572

Aulia, Z. S., Ahmad, T. T., Ayustina, R. R., Hastono, F. T., Hidayat, R. R., Mustakin, H., Fitrianto, A., & Rifanditya, F. B. (2020). Shallow water seabed profile changes in 2016 - 2018 based on Landsat 8 satellite imagery (Case study: Semak Daun Island, Karya Island and Gosong Balik Layar). *Omni-Akuatika*, *16*(3), 26–32. https://doi.org/10.20884/1.oa.2020.16.3.848

Caballero, I., Stumpf, R. P., & Meredith, A. (2019). Preliminary assessment of turbidity and chlorophyll impact on bathymetry derived from sentinel-2A and sentinel-3A satellites in South Florida. *Remote Sensing*, *11*(6), 1–20. https://doi.org/10.3390/rs11060645

Casal, G., Harris, P., Monteys, X., Hedley, J., Cahalane, C., & McCarthy, T. (2020). Understanding satellite-derived bathymetry using Sentinel 2 imagery and spatial prediction models. *GIScience & Remote Sensing*, *57*(3), 271–286. https://doi.org/10.1080/15481603.2019.1685198

Cesbron, G., Melet, A., Almar, R., Lifermann, A., Tullot, D., & Crosnier, L. (2021). Pan-European satellite-derived coastal bathymetry–review, user needs and future services. *Frontiers in Marine Science*, *8*, 1–15. https://doi.org/10.3389/fmars.2021.740830

Chaves, M. E. D., Picoli, M. C. A., & Sanches, I. D. (2020). Recent applications of Landsat 8/OLI and Sentinel-2/MSI for land use and land cover mapping: A systematic review. *Remote Sensing*, *12*(18), Article 3062. https://doi.org/10.3390/rs12183062

Cordeiro, M. C. R., Martinez, J. M., & Peña-Luque, S. (2021). Automatic water detection from multidimensional hierarchical clustering for Sentinel-2 images and a comparison with Level 2A processors. *Remote Sensing of Environment*, *253*, Article 112209. https://doi.org/10.1016/j.rse.2020.112209

Duan, Z., Chu, S., Cheng, L., Ji, C., Li, M., & Shen, W. (2022). Satellite-derived bathymetry using Landsat-8 and Sentinel-2A images: Assessment of atmospheric correction algorithms and depth derivation models in shallow waters. *Optics Express*, *30*(3), 3238–3261. https://doi.org/10.1364/OE.444557

Duplančić Leder, T., Baučić, M., Leder, N., & Gilić, F. (2023). Optical satellite-derived bathymetry: An overview and WoS and Scopus bibliometric analysis. *Remote Sensing*, *15*(5), Article 1294. https://doi.org/10.3390/rs15051294

Ferreira, I. O., Rodrigues, D. D., Santos, G. R. dos, & Rosa, L. M. F. (2017). In bathymetric surfaces: IDW or Kriging? *Boletim de Ciências Geodésicas*, *23*(3), 493–508. https://doi.org/10.1590/s1982-21702017000300033

Hidayat, R. R., Harun, I., Eddiyanto, E., Prihatiningsih, I., & Farabi, A. (2023). Characteristics and dispersion model of wastewater PT

Kayu Lapis Indonesia, Kendal, Central Java. *Journal of Applied Geospatial Information*, *7*(2), 875–882. https://doi.org/10.30871/jagi.v7i2.5841

Jeyar, M., Chaabelasri, E. M., & Salhi, N. (2015). Computational modelling of tidal effect on wastewater dispersion in coastal bays, case of Tangier's bay (Morocco). *Journal of Materials and Environmental Science*, *6*(6), 1715–1718.

Kuhn, C., de Matos Valerio, A., Ward, N., Loken, L., Sawakuchi, H. O., Kampel, M., Richey, J., Stadler, P., Crawford, J., Striegl, R., Vermote, E., Pahlevan, N., & Butman, D. (2019). Performance of Landsat-8 and Sentinel-2 surface reflectance products for river remote sensing retrievals of chlorophyll-a and turbidity. *Remote Sensing of Environment*, *224*, 104–118. https://doi.org/10.1016/j.rse.2019.01.023

Kumaat, J. C., Andaria, K. S., & Maliangkay, D. (2021). Hydro-oceanographic and bathymetric survey in Tanjung Merah as a basis for modelling coastal spatial plans of Bitung City. *E3S Web of Conferences*, *328*, Article 08006. https://doi.org/10.1051/e3sconf/202132808006

Li, S., Wang, X. H., Ma, Y., & Yang, F. (2023). Satellite-derived bathymetry with sediment classification using ICESat-2 and multispectral imagery: Case studies in the South China Sea and Australia. *Remote Sensing*, *15*(4), Article 1026. https://doi.org/10.3390/rs15041026

Lubis, M. Z., Budiana, Gustin, O., Puspita, W. R., Hastuti, A. W., Antoni, S., Rahimah, I., Kausarian, H., & Prasetyo, B. A. (2020). Physical oceanography and hydrodynamic modelling in Tembesi reservoir waters, Batam. In *Proceedings of ICAE 2020 – 3rd International Conference on Applied Engineering* (pp. 1–4), Batam, Indonesia. https://doi.org/10.1109/ICAE50557.2020.9350549

Lyzenga, D. R. (1978). Passive remote sensing techniques for mapping water depth and bottom features. *Applied Optics*, *17*(3), Article 379. https://doi.org/10.1364/ao.17.000379

Lyzenga, D. R. (1985). Shallow-water bathymetry using combined lidar and passive multispectral scanner data. *International Journal of Remote Sensing*, *6*(1), 115–125. https://doi.org/10.1080/01431168508948428

Maslukah, L., Ismunarti, D. H., Widada, S., Sandi, N. F., & Prayitno, H. B. (2022). the interaction of chlorophyll-a and total suspended matter along the Western Semarang Bay, Indonesia, based on measurement and retrieval of Sentinel 3. *Journal of Ecological Engineering*, *23*(10), 191–201. https://doi.org/10.12911/22998993/152428

McFeeters, S. K. (1996). The use of the Normalized Difference Water Index (NDWI) in the delineation of open water features. *International Journal of Remote Sensing*, *17*(7), 1425–1432. https://doi.org/10.1080/01431169608948714

Mudiyanselage, S. S. J. D., Abd-Elrahman, A., Wilkinson, B., & Lecours, V. (2022). Satellite-derived bathymetry using machine learning and optimal Sentinel-2 imagery in South-West Florida coastal waters. *GIScience & Remote Sensing*, *59*(1), 1143–1158. https://doi.org/10.1080/15481603.2022.2100597

Muzirafuti, A., Barreca, G., Crupi, A., Faina, G., Paltrinieri, D., Lanza, S., & Randazzo, G. (2020). The contribution of multispectral satellite image to shallowwater bathymetry mapping on the Coast of Misano Adriatico, Italy. *Journal of Marine Science and Engineering*, *8*(2), Article 126. https://doi.org/10.3390/jmse8020126

Ngoc, D. D., Loisel, H., Jamet, C., Vantrepotte, V., Duforêt-Gaurier, L., Minh, C. D., & Mangin, A. (2019). Coastal and inland water pixels extraction algorithm (WiPE) from spectral shape analysis and HSV transformation applied to Landsat 8 OLI and Sentinel-2 MSI. *Remote Sensing of Environment*, *223*, 208–228. https://doi.org/10.1016/j.rse.2019.01.024

Parente, C., & Vallario, A. (2019). Interpolation of single beam echo sounder data for 3D bathymetric model. *International Journal of Advanced Computer Science and Applications*, *10*(10), 6–13. https://doi.org/10.14569/ijacsa.2019.0101002

Poliyapram, V., Raghavan, V., Metz, M., Delucchi, L., & Masumoto, S. (2017). Implementation of algorithm for satellite-derived bathymetry using open source GIS and evaluation for tsunami simulation. *ISPRS International Journal of Geo-Information*, *6*(3), 1–17. https://doi.org/10.3390/ijgi6030089

Prasetya, M. I., Siregar, V. P., & Agus, S. B. (2023). Comparison of satellite-derived bathymetry algorithm accuracy using Sentinel-2 multispectral satellite image. *Jurnal Kelautan Tropis*, *26*(1), 113–125. https://doi.org/10.14710/jkt.v26i1.16050

Purba, N. P., Faizal, I., Syamsuddin, M. L., Wulandari, A., Bratasena, T., & Therie, R. (2022). Oceanography dataset in Bonpies archipelago as remote island in Java Seas, Indonesia. *Data in Brief*, *40*, Article 107769. https://doi.org/10.1016/j.dib.2021.107769

Rossi, L., Mammi, I., & Pelliccia, F. (2020). UAV-derived multispectral bathymetry. *Remote Sensing*, *12*(23), 1–20. https://doi.org/10.3390/rs12233897

Sagawa, T., Yamashita, Y., Okumura, T., & Yamanokuchi, T. (2019). Shallow water bathymetry derived by machine learning and multitemporal satellite images. In *International Geoscience and Remote Sensing Symposium (IGARSS)* (pp. 8222–8225). IEEE. https://doi.org/10.1109/IGARSS.2019.8899043

Said, N. M., Mahmud, M. R., & Hasan, R. C. (2017). Satellite-derived bathymetry: Accuracy assessment on depths derivation algorithm for shallow water area. *The International Archives of the Photogrammetry, Remote Sensing and Spatial Information Sciences*, *XLII-4/W5*(4W5), 159–164. https://doi.org/10.5194/isprs-archives-XLII-4-W5-159-2017

Seto, M. L., & Crawford, A. (2016). Autonomous shallow water bathymetric measurements for environmental assessment and safe navigation using USVs. In *OCEANS 2015 - MTS/IEEE Washington* (pp. 1–5), Washington, DC, USA. https://doi.org/10.23919/oceans.2015.7404407

Stumpf, R. P., Holderied, K., & Sinclair, M. (2003). Determination of water depth with high-resolution satellite imagery over variable bottom types. *Limnology and Oceanography*, *48*(1), 547–556. https://doi.org/10.4319/lo.2003.48.1_part_2.0547

Wei, J., Wang, M., Lee, Z., Briceño, H. O., Yu, X., Jiang, L., Garcia, R., Wang, J., & Luis, K. (2020). Shallow water bathymetry with multi-spectral satellite ocean color sensors: Leveraging temporal variation in image data. *Remote Sensing of Environment*, *250*, Article 112035. https://doi.org/10.1016/j.rse.2020.112035

Westley, K. (2021). Satellite-derived bathymetry for maritime archaeology: Testing its effectiveness at two ancient harbours in the Eastern Mediterranean. *Journal of Archaeological Science: Reports*, *38*, Article 103030. https://doi.org/10.1016/j.jasrep.2021.103030

Yuliastini, L. F., Zainuri, M., & Widiaratih, R. (2023). Analisis kerentanan pesisir di kabupaten Kendal [Analysis of coastal vulnerability in Kendal regency]. *Indonesian Journal of Oceanography*, *5*(1), 80–89. https://doi.org/10.14710/ijoce.v5i1.16061